THE JOURNAL OF PHYSICAL CHEMISTRY B

Article

pubs.acs.org/JPCB

# Electrophoretic Deposition of Thermites onto Micro-Engineered Electrodes Prepared by Direct-Ink Writing

K. T. Sullivan,* C. Zhu, D. J. Tanaka, J. D. Kuntz, E. B. Duoss, and A. E. Gash

Lawrence Livermore National Laboratory, Livermore, California, United States

**ABSTRACT:** This work combines electrophoretic deposition (EPD) with direct-ink writing (DIW) to prepare thin films of Al/CuO thermites onto patterned two- and three-dimensional silver electrodes. DIW was used to write the electrodes using a silver nanoparticle ink, and EPD was performed in a subsequent step to deposit the thermite onto the conductive electrodes. Unlike conventional lithographic techniques, DIW is a low-cost and versatile alternative to print fine-featured electrodes, and adds the benefit of printing self-supported three-dimensional structures. EPD provides a method for depositing the composite thermite only onto the conductive electrodes, and with controlled thicknesses, which provides fine spatial and mass control, respectively. EPD has previously been shown to produce well-mixed thermite composites which can pack to reasonably high densities without the need for any postprocessing. Homogeneous mixing is particularly important in reactive composities, where good mixing can enhance the reaction kinetics by decreasing the transport distance between the components. Several two- and three-dimensional designs were investigated to highlight the versatility of using DIW and EPD together. In addition to energetic applications, we anticipate that this combination of techniques will have a variety of other applications, which would benefit from the controlled placement of a thin film of one material onto a conductive architecture of a second material.

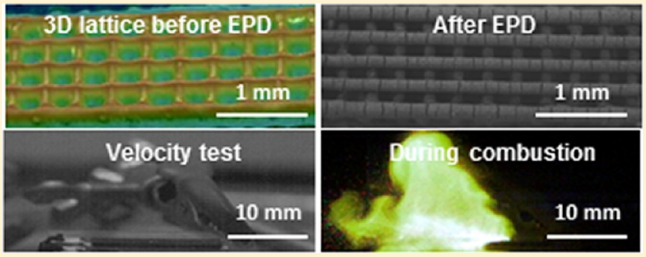


## INTRODUCTION

Electrophoretic deposition (EPD) has received considerable attention for a variety of applications due to its low cost, material diversity, and ease of use. EPD works by dispersing a desired material into a solvent, such as water or ethanol, in which it can acquire a surface charge. The material can then be deposited onto a conductive substrate in the presence of an applied electric field. This most commonly results in a thin film of which the properties, including mass and thickness, can be controlled by the deposition parameters. Due to the wide range of available solvents and operating conditions, the technique has been shown to be suitable for many materials, and also works with different particle sizes and morphologies. Besra et al.[1] have published a thorough review on the fundamentals and applications of EPD.

While most studies have focused on the EPD of a single material, composite materials can also be prepared. This can involve alternating depositions to produce laminate structures[2,3] or, assuming the particles acquire a similar charge in the chosen solvent, this can include the simultaneous codeposition of materials.[3−6] We have recently investigated the latter as a means to prepare well-mixed composite films of Al/CuO thermites onto fine-featured substrates.[7−9] Thermite reactions are those involving a metal fuel and a metal oxide oxidizer, which undergo a high-temperature exothermic reaction upon ignition. Various thermite systems and their relative properties can be found in a publication by Fisher and Grubelich.[10] Two review articles have been published on metal-based energetic materials.[11,12]

One important consideration for thermites is that, in order to achieve a homogeneous and rapid reaction, uniform particle mixing is required. Mixing impacts the kinetics by decreasing the average transport distance between the fuel and oxidizer, and maintaining this mixing throughout the sample is important to ensure the combustion is spatially uniform. It was found that EPD is a well-suited technique for making thermite composites of micrometer-Al/nano-CuO and nano-Al/nano-CuO. The properties of the EPD films, as well as the combustion characterization, can be found in previous works.[7,8] Furthermore, EPD has been used in conjunction with lithographic techniques to deposit thermites directly onto fine-featured (10−1000 $\mu$m) conductive Pt substrates.[9] In this work, a variety of fine-patterned electrodes were utilized to probe various phenomena relevant to microenergetics, such as the ability for thermites to turn corners or jump across gaps. To determine either the reactivity or performance, the as-deposited material was locally ignited, and the self-propagating flame was imaged using a high-speed camera. Patterned electrodes may be useful in applications such as microenergetics,[13,14] where precision placement of the reactive material is necessary for ensuring the functionality of the device. As an example, we examined the ability of using thermites for multichannel

**Special Issue:** B: Electrophoretic Deposition

**Received:** June 29, 2012
**Revised:** August 14, 2012
**Published:** August 16, 2012

   dx.doi.org/10.1021/jp306440t | J. Phys. Chem. B 2013, 117, 1686−1693

ignition, in which a single ignition point splits into six equidistant channels.[9] This was made by first printing the electrode using lithography (sputter-deposited Pt with a strip width of 250 $\mu$m), and then using EPD to deposit a thin film of the thermite onto the Pt. We found that the ignition delay could be tailored by changing either the particle size or the fuel/oxidizer ratio, and that the timing of the six channels exhibited very good performance, <5% uncertainty in the arrival time.

One drawback of using lithographic techniques is that they can be costly and time-consuming. Furthermore, lithography is currently limited to two-dimensional designs. Direct-ink writing (DIW) is a relatively new technique which has emerged for printing of materials into two- and three-dimensional architectures.[15−21] Inks are high-volume fraction loaded dispersions of a candidate material, which are often particles, but can include other formulations such as sol−gel precursors.[22] The ink is flowed through a fine-tipped nozzle by applying either constant pressure or constant displacement, and a sample is moved using a multiaxis stage to form the desired pattern. If the rheological properties are tuned correctly, the ink can undergo shear-thinning upon flow through the nozzle, and solidification upon exiting, thus allowing it to retain its filamentary shape. Because of this attribute, self-supporting three-dimensional structures can be printed with fine features within. The feature size can range from submicrometer to much larger, and is a function of several parameters, including particle size, nozzle size, print speed, pressure, etc.

While DIW could potentially be used to directly write thermite inks, in this work, we focus on using DIW to print silver conductive electrodes. EPD is then performed in a subsequent step to deposit the thermite. This combination of techniques allows for a wide range of architectures to be prepared, which include the DIW conductive substrate coated with a thermite using EPD. The main goal of this study is to introduce this combination of techniques, and to explore the design space to examine what types of patterns and structures can be produced. We expect that this method will find use in several other applications besides energetic materials, in particular where a thin film of one material (or composite) deposited onto a pattern or structure of a second material would be advantageous.

## EXPERIMENTAL SECTION

The CuO used was Nanotek (Nanophase, Inc.), and had a primary particle size of <50 nm as determined using electron microscopy. Micron-Al was purchased from Valimet (H-2), and had a particle size of 3.2 $\mu$m, as specified by the supplier. Nano-Al was purchased from Novacentrix, and had a specified particle size of 80 nm. Al acquires a few nanometer thick passivating amorphous oxide shell ($Al_2O_3$) when exposed to air, and this needs to be accounted for in weighing, especially as the particle size is decreased and the shell represents a larger fraction of the mass. For the nano-Al in this work, the oxide shell represents 27% of the mass, determined by using thermogravimetric analysis (TGA, 25−1000 °C at 5 °C/min in dry air). The reported size for the nanoparticles is that of the primary particles, but it should be noted that there are varying amounts of aggregation. This is important to note because, in combustion measurements of nanoparticles, it is not yet clear whether the primary particle or the aggregate size is a more appropriate metric to consider.

The equivalence ratio is defined as the molar ratio of fuel to oxidizer relative to that in the stoichiometric reaction:

$$\Phi = \frac{(F/O)_{actual}}{(F/O)_{stoich}}$$

The stoichiometric reaction is given as

$$2Al + 3CuO \rightarrow Al_2O_3 + 3Cu$$

The amount of aluminum was adjusted to account for only the elemental portion when weighing samples. It is important to distinguish between the equivalence ratio in the precursor dispersion and that in the as-deposited film. If the two materials deposit at different rates (i.e., they have different charges in the desired solvent), then the ratio in the as-deposited film will be different from the starting mixture. This is especially important to consider in thermites, because there is an equivalence ratio which gives rise to the highest reactivity, and accurately knowing this value is often useful to help understand the reaction mechanism. We have reported the optimum equivalence ratio after deposition, which yields the fastest flame propagation velocity, was $\Phi = 1.6 \pm 0.2$ and $\Phi = 1.7 \pm 0.2$ for micrometer-Al/nano-CuO[7] and nano-Al/nano-CuO[8] thermites, respectively. These are both fuel-rich formulations, meaning that excess Al can help enhance the reactivity. There are a variety of reasons excess Al could be beneficial to the reactivity, and we have suggested some possibilities in previous work.[7,8] In the current work, all studies are done using the optimum value of equivalence ratio.

The dispersions for EPD were prepared using a previous method,[7,8] with a total solids loading of 0.2 vol % in a 3:1 EtOH:$H_2O$ solution. The corresponding amount of Al and CuO were weighed and added to a 50 mL centrifuge tube along with 30 mL of EtOH (200 proof). The dispersion was ultrasonicated for 60 s using a tip sonicator (Branson 250, 200 W power) operating at full power and 50% duty cycle. The dispersion was stirred and sonicated for an additional 60 s, followed by the addition of 10 mL of water. We chose to add the water after the sonication step to mitigate potential oxidation of the Al. Al will oxidize in water if given sufficient time, so extended storage is not possible. However, we found that the active content of Al remained unchanged for at least 8 h, thus allowing sufficient time to complete the depositions in this work.

Silver nanoparticle inks were prepared following a previous method,[19] which involves the reduction of a metal precursor in solution in the presence of a surface capping agent. An aqueous silver nitrate precursor solution was used, with poly(acrylic acid) (PAA) as the capping agent and diethanolamine (DEA) as the reducing agent. Acetone or ethanol was added to induce rapid particle coagulation, followed by centrifugation to achieve a highly concentrated ink (≥70 wt %). Ethylene glycol was then added as a humectant, which keeps the ink from drying in air.

The as-prepared silver nanoparticle ink was loaded into a syringe with a 200 $\mu$m inner diameter nozzle (Nordson EFD). A glass substrate ($27 \times 27 \times 0.525$ mm$^3$) was placed on a three-axis positioning stage (Aerotech), above which the syringe is mounted. The pressure was then increased to the desired value, and the positioning stage was controlled via the Aerotech software to produce the desired pattern. After printing, the substrates were heated to 350 °C in air for 1 h to drive off the organics and partially sinter the nanoparticles, thus rendering conductive silver to be used as an electrode for EPD. It should


dx.doi.org/10.1021/jp306440t | J. Phys. Chem. B 2013, 117, 1686−1693

be noted that various parameters, both of the ink and the writing process, can be changed to tune the dimensions of the as-written features. The nozzle height, nozzle diameter, print speed, pressure, and viscosity of the ink are just some attributes which can affect the size and morphology of the written filaments. The finest features patterned thus far using DIW were $TiO_2$ filaments of ~250 nm in width, which were printed using a sol–gel based ink.[22] For many nanoparticle-based inks, the feature sizes are bigger because the nozzle must be significantly larger (~100×) than the size of the particles to prevent clogging. The features studied in this work, although small, are sufficiently larger than the diameter in which clogging becomes an issue.

If three-dimensional structures are desired, then the strategy is to match the printing speed to the ink gelation rate. If done correctly, the ink will solidify as it exits the nozzle, thus allowing it to retain its filamentary shape. Three-dimensional architectures can then be designed and printed, as long as the structures can support their own weight. A schematic of the DIW process, along with examples of two- and three-dimensional electrodes, are shown in Figure 1.

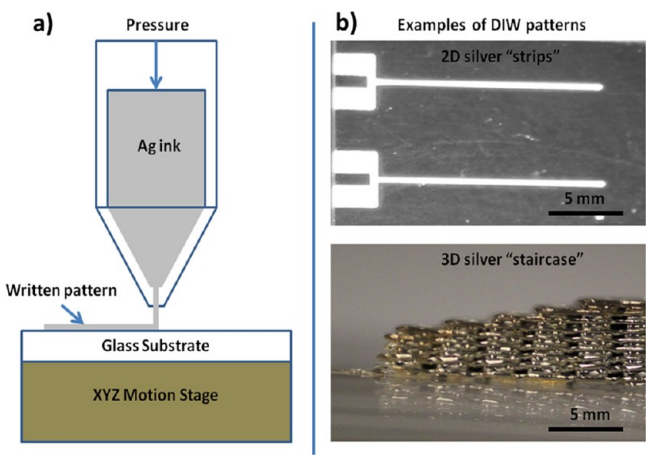


**Figure 1.** (a) Schematic of the DIW process for printing silver electrodes. Also shown are two examples of the types of electrodes which can be printed (b). Three-dimensional structures are possible, as long as the structure can be supported by the underlying layers. The "U" shaped sections are where the reaction is initiated via a fast current pulse.

EPD was performed using a custom-built cell, which uses 27 × 27 $mm^2$ electrodes, ~1 mm thick. The spacing between the electrodes is 1 cm, and the cell has a free volume of ~7 mL. The infill rate was 10 mL/min, controlled by a syringe pump. After filling, with the cell oriented vertically, the cell was turned horizontally so that the deposition electrode was on top. While the orientation of the cell may not affect the deposition, we choose this method to prevent any settling of material from the dispersion onto the substrate. Both Al and CuO acquired a positive charge in the chosen solvent, and thus deposit on the cathode. A DC voltage was applied for a prescribed amount of time and then the voltage was turned off and the dispersion immediately withdrawn at a rate of 2 mL/min. After the dispersion was removed, the electrodes were dried upright under a small glass cover, which slows the drying rate and helps reduce delamination of the deposit. An example of the combined DIW + EPD technique is shown in Figure 2.

Images were taken using an optical microscope (Eclipse 80i, Nikon Corp., Plan Apo 2×, N. A. 0.1), or a digital microscope imaging system (VHX-1000, Keyence Corp.), which collects a series of images at varying heights, and then uses software analysis to render a three-dimensional object with height displayed as a colored topographic map. Combustion analysis is performed by igniting the thermite and imaging the self-propagating flame using a high-speed CCD camera (Phantom, Vision Research Inc.). Ignition was achieved using a pulsed power supply to resistively heat the built-in igniter section. The igniter can be seen as the "U" shaped pad on the left side of the strip electrode shown in Figures 1 and 2. If the material could not be ignited using this technique, a Tesla coil was used, and was not observed to impact the velocity. The high-speed images can either be used for mechanistic investigations, such as examining the flame velocity as a function of film thickness, or can be used to evaluate other behavior, such as the use of thermites for microenergetic timing delay generators.[9] An example of a combustion event is shown in Figure 3, which was nano-Al/nano-CuO ($\Phi$ = 1.7) imaged at 100 000 frames per second. The linear velocity is calculated from the image sequence by measuring the time difference for the flame to travel a fixed distance (~15 mm). In Figure 3, the measured flame propagation velocity is 43 m/s.

## RESULTS AND DISCUSSION

As mentioned previously, the equivalence ratio is a critical parameter when discussing the combustion phenomena. Not only is it beneficial to know the optimized mixture from an application standpoint, the peak ratio is also useful to help elucidate the underlying combustion mechanism. We found that inductively coupled plasma optical emission spectroscopy (ICP-OES, PerkinElmer Optima 4300DV) could accurately determine the equivalence ratio in the as-deposited films. The details of this analysis can be found elsewhere.[7,8] The equivalence ratio measured using ICP-OES ($\Phi_{deposited}$) was plotted as a function of the equivalence ratio weighed in the dispersion ($\Phi_{weighed}$), and the results are shown in Figure 4. As can be seen, the scaling is linear over the range of equivalence ratios used in this work. This behavior indicates that the deposition rate is directly proportional to the concentration of each species within this range of conditions. The slope of the data can be used to correlate the weighed equivalence ratio to that in the deposited film. As can be seen, the micrometer-Al/nano-CuO exhibits nearly a 1:1 correlation, meaning that the Al and CuO in this case deposit at similar rates. The nano-Al/nano-CuO, however, exhibits a smaller constant of proportionality. This implies that the nano-Al deposits at a lower rate than the nano-CuO and, thus, the concentration of nano-Al in the dispersion must be increased accordingly in order to yield the desired equivalence ratio in the deposit. For all combustion studies, $\Phi_{weighed}$ is selected to yield $\Phi_{deposited}$ = 1.6 and $\Phi_{deposited}$ = 1.7 for the micrometer-Al and nano-Al thermites, respectively, corresponding to their optimum values of reactivity.

The combination of DIW and EPD opens up many possibilities for designing and placing thin films of material onto or into two- and three-dimensional architectures. In order to better understand the reaction mechanism, we have explored a wide variety of designs, some early results of which are reported here. For thermites, there are several simultaneous parameters which may affect the propagation rate. These parameters include, but are not limited to, particle size,

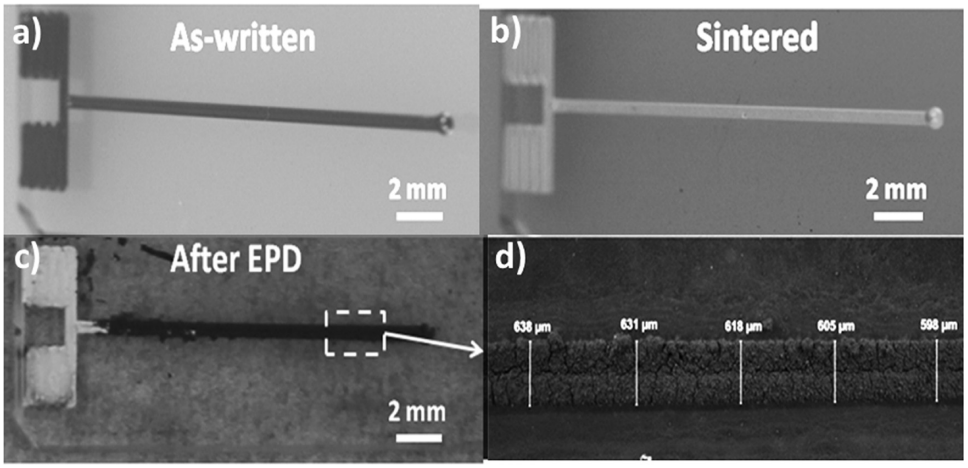


**Figure 2.** Schematic showing the combination of DIW + EPD. A desired pattern is printed using a Ag ink (a). The ink is then thermally treated to convert it into conductive silver (b). The electrode is then used with EPD to deposit the thermite onto the pattern (c and d).

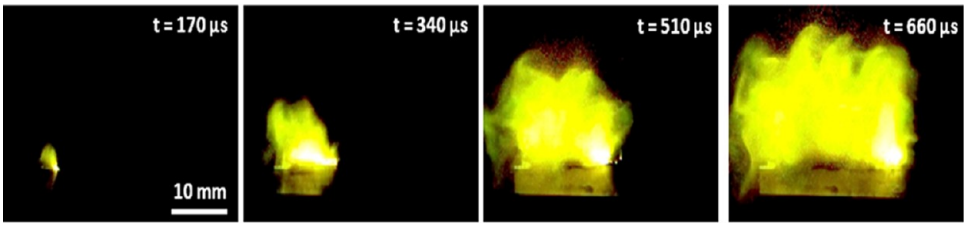


**Figure 3.** Image sequence from the combustion of optimized nano-Al/nano-CuO. The frame rate was 100 000 frames per second, and the measured flame velocity was 43 m/s.

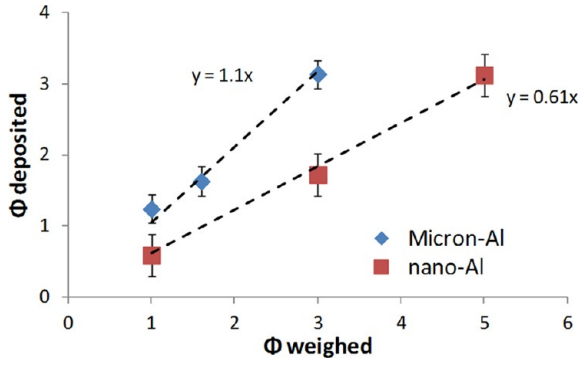


**Figure 4.** Relationship between the weighed equivalence ratio in the dispersion and that in the as-deposited thermite film (measured using ICP-OES).

morphology, density, interfacial contact, adiabatic flame temperature, melting temperature, gas generation, heating rate, and equivalence ratio. The presence of so many variables makes it challenging to isolate the effects of any one variable on the reactivity. For example, a study which changes the particle size will also change the heating rate, interfacial contact, and melting temperature, if small enough particles are used. This codependence of parameters is something which in most cases cannot be avoided, and complicates the analysis. That being said, much can be learned from experiments which are designed to investigate a single parameter while fixing as many other parameters as possible.

One example of an experiment which minimizes the number of changing parameters is shown in Figure 5. Here, two-dimensional silver patterns are first written using DIW, and then coated with a thin film (~40 $\mu$m) of micrometer-Al/nano-CuO. After deposition, the effective width of the thermite on the strips is approximately 400 $\mu$m with a 200 $\mu$m void in between adjacent strips (see Figure 5b). Before the patterned section, an unpatterned section is also included to acquire a reference velocity. In all examples, the flame propagates for 10 mm down the unpatterned section, and then encounters the patterned regime. The intent is to investigate the effects of void orientation on the combustion velocity. A recent work was performed by Parimi et al.[23] for porous Si energetics, in which the authors probed the effects of ordered microstructures on the propagation velocity, and found a large enhancement for certain configurations of micrometer-scale pillars patterned onto a base of the energetic material. A large component of the reaction mechanism for thermites involves the energy transport through the material, and thus, we sought to determine whether the void orientation would impact the flame velocity. It should be noted that the perpendicular and 45° patterns in Figure 5 would ideally not be connected at the top and bottom; however, they needed to be written this way to make the entire structure conductive for EPD. In the videos, the flame could be seen to jump the gaps, and thus, we expect the edges did not significantly impact the results.

For these studies, we measured no difference in flame velocity between the patterned and unpatterned regions, which both propagated with velocities of around 1.5 m/s. For such slow velocities, the dominant mode of energy transport has been suggested to be via conduction. Therefore, it is interesting that the flame does not slow down in the patterned regimes. This result suggests that conductive heat transfer in such materials does not occur through the solid particles but must occur through the gases, either the intermediate combustion gases or the existing interstitial gases. Alternatively, this result


dx.doi.org/10.1021/jp306440t | J. Phys. Chem. B 2013, 117, 1686−1693

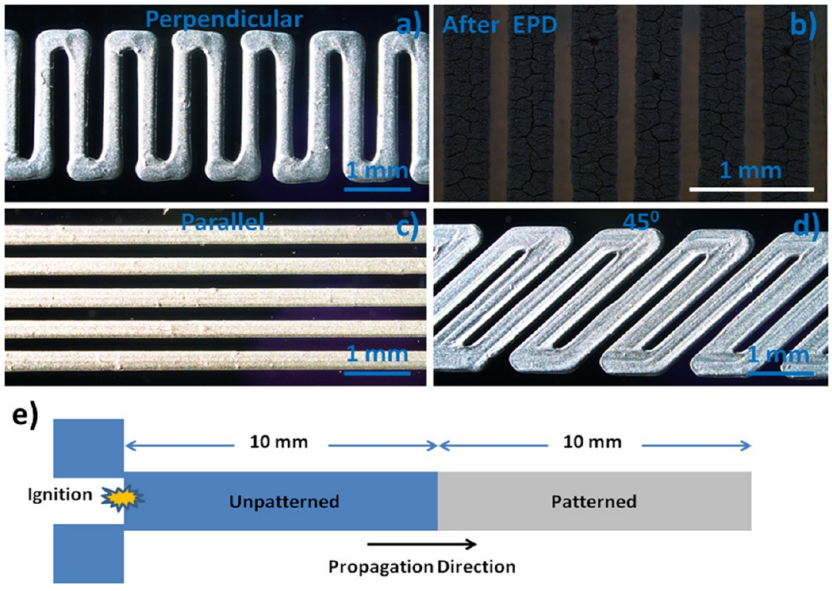


**Figure 5.** Silver patterns used to look at the effects of void orientation on flame propagation velocity (a, c, d). Also shown is a high magnification image (b) after a deposition onto the perpendicular electrode (a). In all cases, the reaction proceeds from left to right (e), and the voids are thus oriented parallel, perpendicular, or 45° to the direction of propagation.

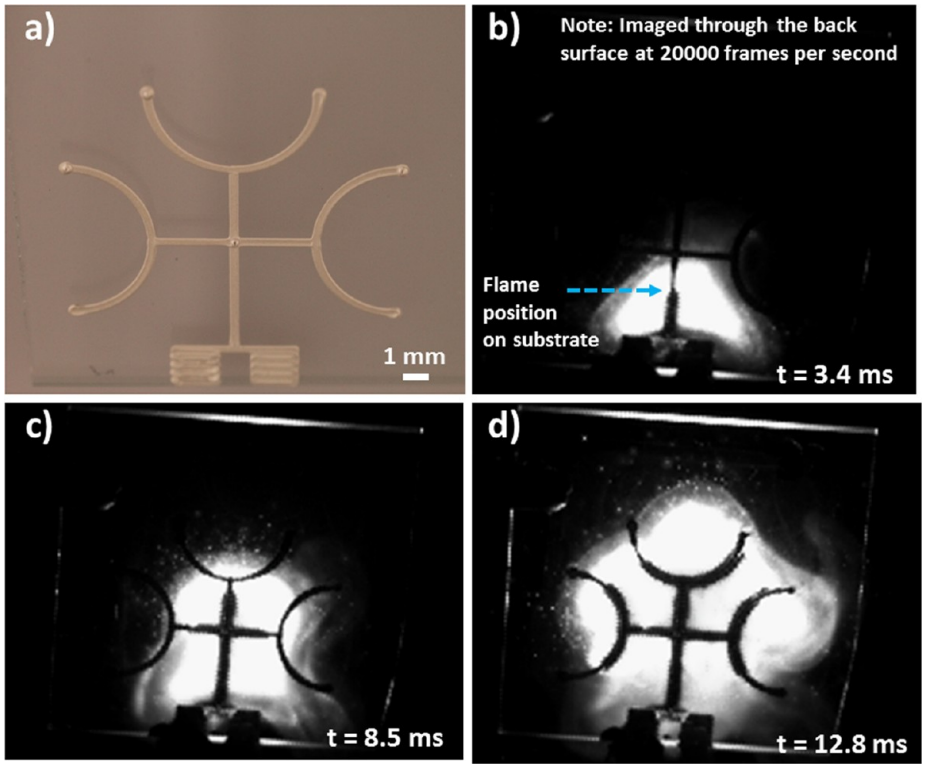


**Figure 6.** Multichannel ignition achieved from a single ignition point. The pattern before deposit is shown in part a, and the flame is imaged through the back surface of the glass (b–d). As the reaction occurs, it leaves a dark residue, allowing for tracking of the flame position. The arrival time of the flame at the six channels was measured and the uncertainty used to quantify the fidelity of this device for potential applications.

could suggest that a mechanism besides conduction is controlling the propagation, even at slow velocities. One possibility is that particle advection occurs as intermediate gases are generated, and this serves to transport molten particles forward, which can transfer energy if they come into contact with unreacted material in the propagation direction. This has also been suggested for Al/MoO3 burning in microchannels, which propagate at much faster velocities.[24] The authors suggested that the molten Mo product could be transported forward and could condense onto unreacted material, thus assisting the effective energy transport. We have also observed the advection of particles in a recent work involving nano-Al/nano-CuO thermites.[8] It is not known how relevant advection is for the micrometer-Al/nano-CuO composite studied here, and for such slowly propagating flames. However, if it is occurring, then we would expect the void orientation would not


dx.doi.org/10.1021/jp306440t | J. Phys. Chem. B 2013, 117, 1686–1693

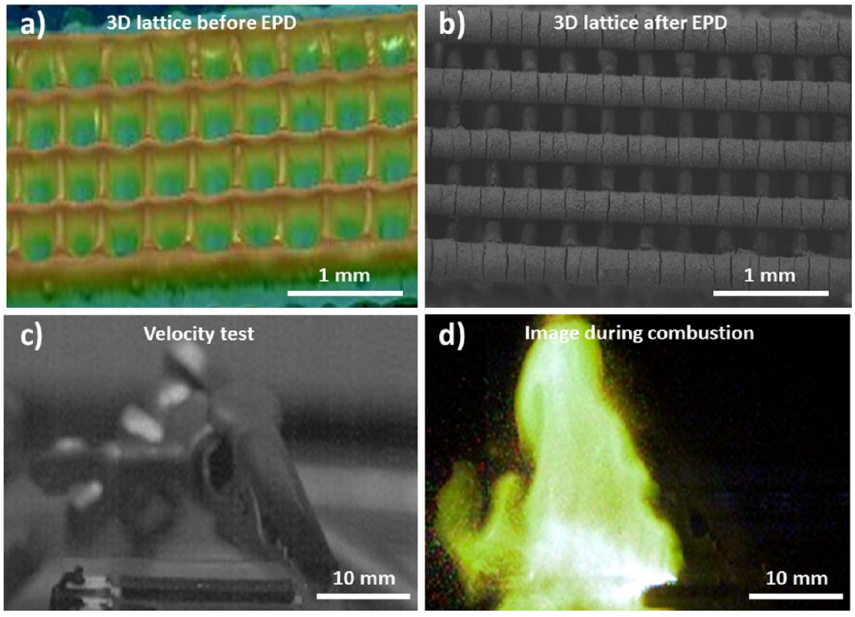


**Figure 7.** Example of a three-dimensional lattice used as an electrode for EPD of a thermite. (a) Image taken using a digital microscope capable of reconstructing a three-dimensional object. Other images are before (b, c) and during (d) combustion.

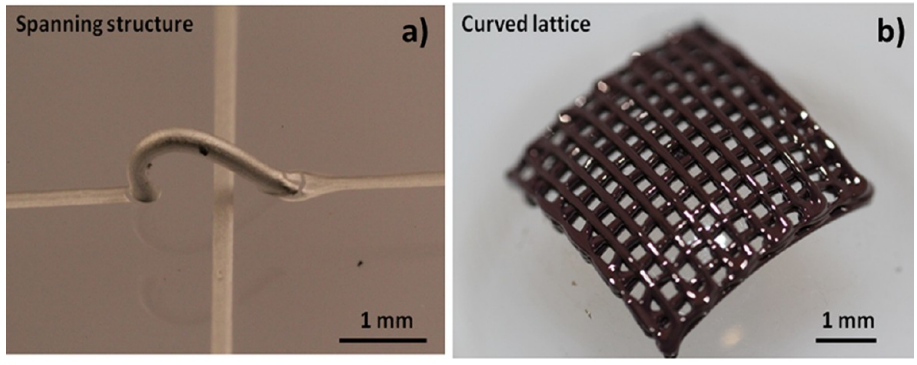


**Figure 8.** Two examples of three-dimensional silver electrodes printed using DIW. The left example (a) highlights the ability to print a bridge over an underlying feature, and the right (b) shows the ability to print onto curved surfaces. The structures can then be removed to render a free-standing curved electrode.

impact the flame velocity, assuming that the particles have enough inertia to cross the distance of the gaps while remaining hot enough to ignite the material on the other side.

In addition to the mechanistic studies, there are many potential applications which could benefit from controlled placement of an energetic material using DIW + EPD. One example already discussed is microenergetic applications, where incorporating the energetic material into or onto a small device becomes challenging as the size decreases. We have recently investigated using lithographically patterned electrodes with EPD for microenergetic characterization,[9] and showed an example of an electrode design which could be used as a tunable multichannel igniter. In the current work, we have repeated this design but in this case have used DIW to print the electrode. The performance was characterized by measuring the average time for the flame to transit from the ignition point to the six end points in the device, and the uncertainty is quantified by calculating the standard deviation of the six data points, and dividing this by the average arrival time to express this value as a percentage. An example of the electrode, along with images from the combustion, is shown in Figure 6. This particular example is micrometer-Al with nano-CuO, and has an average arrival time of 14.7 ms with 4.8% uncertainty in the six channels. While the features of the silver electrodes are not as high precision as lithography, we find DIW to be a suitable method for making such electrodes. This is done at a fraction of the cost, and with the added versatility of changing designs, without the need to make a new mask each time.

As mentioned, one other clear advantage of using DIW over lithography is that three-dimensional electrodes can be built, assuming that the ink and pattern are designed to support the weight of the structure. An example of a three-dimensional lattice is shown in Figure 7. This design is written by stacking two-dimensional serpentine patterns on top of one another, with each alternating layer oriented 90° to the layer below it. Both the filament width and spacing can be controlled to result in an electrode which has ordered pores in three dimensions. A design like this may be useful for a variety of nonenergetic applications; for example, those which desire to couple gas transport into a structure with the surface activity of a thin film. For the current work, such structures are mainly being investigated to determine if the architecture can be utilized to tailor the reactivity. It has been speculated that thermites transport energy via convection of intermediate and/or product


dx.doi.org/10.1021/jp306440t | J. Phys. Chem. B 2013, 117, 1686−1693

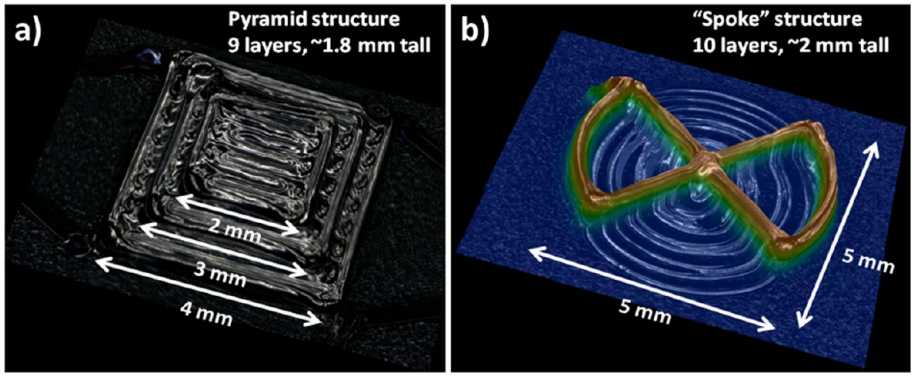


**Figure 9.** Examples of three-dimensional shaped electrodes printed using DIW. Shown is a pyramid structure (a) along with a spoke structure (b).

gases,[25−28] and thus, we anticipate that using a three-dimensional network with designed conduits for gas transport may enhance the energy propagation. This is currently being investigated in much more detail, but preliminary results are included here mainly to demonstrate the ability to synthesize three-dimensional architectures which incorporate energetic materials.

In addition to mechanistic studies, three-dimensional electrodes can potentially be used for a variety of applications. Two examples are shown in Figure 8. This includes using the silver ink to suspend an electrode over an existing feature, without making contact. This is applicable to microenergetic applications if, for example, the energetic material needs to be incorporated without perturbing an existing feature, such as an electronic circuit. Upon EPD, the thermite can be seen to wrap around the silver filament, thus suspending an energetic film above the underlying feature. The second example is a three-dimensional silver lattice (image shown is before heat treatment) which was written onto a curved surface and then removed. DIW can accommodate any arbitrary surface, so long as the transition stage has a sufficient number of degrees of freedom to move the part and print the desired pattern. EPD can then be performed on such parts, assuming that a conductive pathway is made. The curved lattice demonstrates the ability to print directly onto cylindrical or spherical surfaces or, also, to print onto these surfaces and then remove the structures to make a free-standing curved part.

One other type of three-dimensional electrode we have printed using DIW is shaped electrodes. Two examples of this are shown in Figure 9, and include a three-layer pyramid, along with a cylindrical structure. Shaped electrodes like this could be useful to control the morphology of EPD films, which will conform to the surface of the electrode. One potential application is to use the electrode morphology to shape the resultant flame, as was observed in preliminary tests. Thermite flame shaping could be useful for a variety of applications, including micropropulsion, igniters, welding, or cutting, to name a few.

## CONCLUSIONS

This work combined direct-ink writing with electrophoretic deposition to prepare architectures of thermite composite films. This particular combination of techniques is low-cost and versatile, compared with lithographic techniques. Furthermore, DIW allows for the design of self-supported three-dimensional electrodes, thus greatly expanding the application space for using EPD. The equivalence ratio was first investigated to determine how the fuel/oxidizer ratio in the dispersion translated into that in the as-deposited film. A linear relationship was observed, indicating that the deposition rate scales directly with concentration within the range of experimental conditions used. The relative amount of fuel and oxidizer in the dispersion can thus be adjusted to produce the desired equivalence ratio in the EPD film.

Several two- and three-dimensional silver electrodes were printed using DIW. Some were intended to investigate the reaction mechanism, while others were designed more from an application standpoint. The selection of results was intended to highlight the overall versatility of combining these two techniques. In addition to energetic applications, we suspect these techniques will find a variety of applications in nonenergetic applications.

## AUTHOR INFORMATION

### Notes

The authors declare no competing financial interest.

## ACKNOWLEDGMENTS

The authors would like to thank Franco Gagliardi for his help with the three-dimensional imaging. We would also like to acknowledge Doug Hahn for his assistance with the high-speed camera setup. Thanks to Thomas Fitch and the waste treatment group in the radioactive and hazardous waste management program for conducting the ICP-OES measurements. This work was funded by the Laboratory Directed Research and Development Strategic Initiative program, Disruptive Fabrication Technologies Initiative 11-SI-005, and performed under the auspices of the U.S. Department of Energy by Lawrence Livermore National Laboratory under Contract DE-AC52-07NA27344.

## REFERENCES

(1) Besra, L.; Liu, M. *Prog. Mater. Sci.* **2007**, *52*, 1−61.
(2) Hadraba, H.; Klimes, J.; Maca, K. *J. Mater. Sci.* **2007**, *42*, 6404−6411.
(3) Hadraba, H.; Maca, K.; Cihlar, J. *Ceram. Int.* **2004**, *30*, 853−863.
(4) Ferrari, B.; Santacruz, I.; Nieto, M. I.; Moreno, R. *J. Eur. Ceram. Soc.* **2004**, *24*, 3073−3080.
(5) Lin, T. H.; Huang, W. H.; Jun, I. K.; Jiang, P. *Electrochem. Commun.* **2009**, *11*, 1635−1638.
(6) Wang, Y. H.; Chen, Q. Z.; Cho, J.; Boccaccini, A. R. *Surf. Coat. Technol.* **2007**, *201*, 7645−7651.
(7) Sullivan, K. T.; Worsley, M. A.; Kuntz, J. D.; Gash, A. E. *Combust. Flame* **2012**, *159*, 2210−2218.

(8) Sullivan, K. T.; Kuntz, J. D.; Gash, A. E. *J. Appl. Phys.* **2012**, *112*, 024316-1−024316-12.
(9) Sullivan, K. T.; Kuntz, J. D.; Gash, A. E. *International Journal of Energetic Materials and Chemical Propulsion* **2012**, submitted for publication.
(10) Fischer, S. H.; Grubelich, M. C. *24th Int Pyrotechnics Seminar*, Monterey, California, 1998, pp 1−13.
(11) Piercey, D. G.; Klapotke, T. M. *Cent. Eur. J. Energ. Mater.* **2010**, *7*, 115−129.
(12) Dreizin, E. L. *Prog. Energy Combust. Sci.* **2009**, *35*, 141−167.
(13) Tappan, A. *15th APS Topical Conference on Shock-Compression of Condensed Matter*, Kohala Coast, HI, 2007, pp 997−1002.
(14) Rossi, C.; Esteve, D. *Sens. Actuators, A* **2005**, *120*, 297−310.
(15) Lewis, J. A. *Adv. Funct. Mater.* **2006**, *16*, 2193−2204.
(16) Lewis, J. A.; Smay, J. E.; Stuecker, J.; Cesarano, J. *J. Am. Ceram. Soc.* **2006**, *89*, 3599−3609.
(17) Simon, J. L.; Michna, S.; Lewis, J. A.; Rekow, E. D.; Thompson, V. P.; Smay, J. E.; Yampolsky, A.; Parsons, J. R.; Ricci, J. L. *J. Biomed. Mater. Res., Part A* **2007**, *83A*, 747−758.
(18) Xu, M. J.; Gratson, G. M.; Duoss, E. B.; Shepherd, R. F.; Lewis, J. A. *Soft Matter* **2006**, *2*, 205−209.
(19) Ahn, B. Y.; Duoss, E. B.; Motala, M. J.; Guo, X. Y.; Park, S. I.; Xiong, Y. J.; Yoon, J.; Nuzzo, R. G.; Rogers, J. A.; Lewis, J. A. *Science* **2009**, *323*, 1590−1593.
(20) Ahn, B. Y.; Lorang, D. J.; Lewis, J. A. *Nanoscale* **2011**, *3*, 2700−2702.
(21) Adams, J. J.; Duoss, E. B.; Malkowski, T. F.; Motala, M. J.; Ahn, B. Y.; Nuzzo, R. G.; Bernhard, J. T.; Lewis, J. A. *Adv. Mater.* **2011**, *23*, 1335−1340.
(22) Duoss, E. B.; Twardowski, M.; Lewis, J. A. *Adv. Mater.* **2007**, *19*, 3485−3489.
(23) Parimi, V. S.; Tadigadapa, S. A.; Yetter, R. A. *J. Micromech. Microeng.* **2012**, *22*, 055011-1−055011-6.
(24) Son, S. F.; Asay, B. W.; Foley, T. J.; Yetter, R. A.; Wu, M. H.; Risha, G. A. *J. Propul. Power* **2007**, *23*, 715−721.
(25) Dean, S. W.; Pantoya, M. L.; Gash, A. E.; Stacy, S. C.; Hope-Weeks, L. J. *J. Heat Transfer* **2010**, *132*, 111201.
(26) Malchi, J. Y.; Yetter, R. A.; Foley, T. J.; Son, S. F. *Combust. Sci. Technol.* **2008**, *180*, 1278−1294.
(27) Asay, B. W.; Son, S. F.; Busse, J. R.; Oschwald, D. M. *Shock Compression of Condensed Matter* - **2003**, *Pts 1 and 2, Proceedings* **2004**, *706*, 827−830.
(28) Sanders, V. E.; Asay, B. W.; Foley, T. J.; Tappan, B. C.; Pacheco, A. N.; Son, S. F. *J. Propul. Power* **2007**, *23*, 707−714.